Phenomenology of Neutrino Oscillations

G.L. Fogli[a], E. Lisi[a*], A. Marrone[a], D. Montanino[b], and A. Palazzo[a]

[a]Dipartimento di Fisica and Sezione INFN di Bari, Via Amendola 173, 70126 Bari, Italy

[b]Dipartimento di Fisica and Sezione INFN di Lecce, Via Arnesano, 73100 Lecce, Italy

We review the status of several phenomenological topics of current interest in neutrino oscillations: (i) Solar neutrino oscillations after the first Sudbury Neutrino Observatory measurements, including both model-independent and model-dependent results; (ii) Dominant $\nu_\mu \to \nu_\tau$ oscillations of atmospheric and K2K neutrinos, and possible subdominant oscillations induced by either extra states or extra interactions; and (iii) Four-neutrino scenarios embedding the controversial LSND evidence for oscillations.

1. INTRODUCTION

Evidence in favor of ν oscillations is accumulating at a fast rate. The strong evidence for disappearance of atmospheric ν_μ in Super-Kamiokande (SK) [1], consistent with the μ spectrum anomaly in MACRO [2] and with Soudan-2 (μ, e) data [3], is successfully explained by $\nu_\mu \to \nu_\tau$ oscillations. The recent data from the first long-baseline K2K experiment [4] also support such an interpretation [5]. The global evidence for solar ν_e oscillations from radiochemical (Cl and Ga) [6,7] and Cherenkov (SK and SNO) detectors [8] is strongly corroborated (at a significance level $> 3\sigma$ [9]) by the comparison of the recent SNO data [10,11] with those collected in SK [12].

We review "established" aspects of the above pieces of evidence, as well as (partially) "unsolved" issues concerning sterile neutrinos, new neutrino interactions, and the controversial $\nu_\mu \to \nu_e$ signal in LSND [13].

2. SOLAR NEUTRINOS AFTER SNO

The main goal of the SNO heavy-water experiment is to measure the solar neutrino flux both in charged current mode

$$\nu_e + d \to p + p + e^- \ (\mathrm{CC}) \ ,$$

sensitive to ν_e only, and in neutral current mode

$$\nu_x + d \to p + n + \nu_x \ (\mathrm{CC}) \ ,$$

sensitive to any active flavor $\nu_x = \nu_{e,\mu,\tau}$. A suppression of the CC/NC ratio is expected in the presence of $\nu_e \to \nu_x$ oscillations. The first CC data have recently been released [10], while the NC measurement is still in progress [8].

The SK experiment is also sensitive to CC and NC reactions through elastic scattering on e^-,

$$\nu_x + e^- \to \nu_x + e^- \ (\mathrm{ES}) \ ,$$

but no discrimination is possible for the event type (CC or NC). However, one can indirectly use the SNO CC measurement to "extract" a possible NC component in SK. Indeed, this component turns out to be nonzero at $> 3\sigma$ level, indicating that $\nu_e \to \nu_{\mu,\tau}$ transitions are occurring.

2.1. Model-independent implications

Assuming active ν oscillations, the main unknowns for the calculations of the SNO CC rate are the ν_e survival probability averaged over the detector response function, $\langle P_{ee} \rangle_{\mathrm{SNO}}$, and the ratio f_B of the absolute ^{8}B spectrum to the reference one estimated in the Standard Solar Model (SSM) of [14]. Analogously, the unknowns associated to the SK ES rate are $\langle P_{ee} \rangle_{\mathrm{SK}}$ and f_B. The two available data (SNO CC and SK ES rates) are insufficient to pin down three unknowns $[\langle P_{ee} \rangle_{\mathrm{SNO}}, \langle P_{ee} \rangle_{\mathrm{SK}}, f_B]$, unless one make some hypothesis on either the SSM (e.g., by setting $f_B = 1$), or the oscillation model [e.g., by setting a functional form of $P_{ee}(E_\nu)$)].

However, it has been shown in [15,16] that, by appropriately shifting the SK energy thresh-

*Speaker. E-mail: eligio.lisi@ba.infn.it

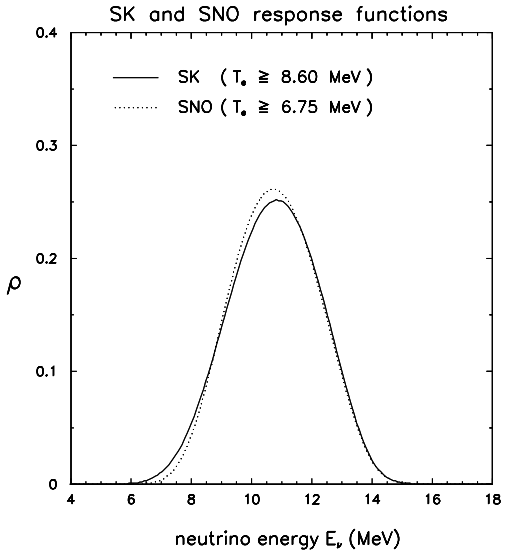

Figure 1. SNO response function for neutrino-induced CC events with $T_e > 6.75$ MeV (dotted curve), and equalized SK response function for ES events with $T_e > 8.60$ MeV (solid curve) [17].

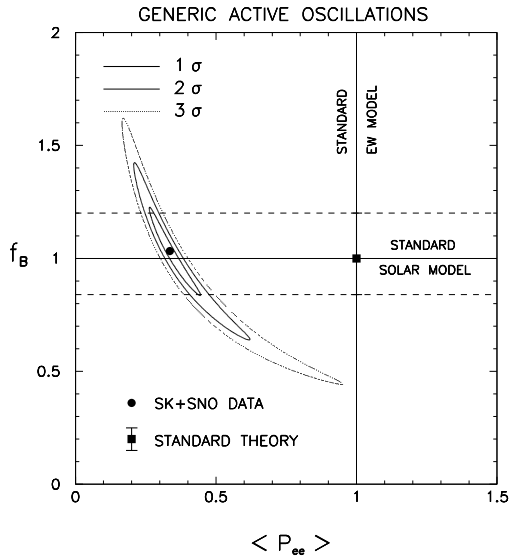

Figure 2. SK+SNO combined constraints on f_B and $\langle P_{ee}\rangle$. Preferred values are $f_B \sim 1$ (in agreement with the standard solar model) and $P_{ee} \sim 1/3$ (inconsistent with the hypothesis of no oscillations) [17].

old, one can reach an accurate "equalization" of the SK and SNO response as a function of the neutrino energy. For the current SNO threshold in electron kinetic energy (6.75 MeV), the SK threshold providing the best equalization is 8.60 MeV, as shown in Fig. 1 [17].

This lucky circumstance implies that the SNO CC and SK ES experiments, above such thresholds, are sensitive to the *same* energy-averaged survival probability P_{ee},

$$\langle P_{ee}\rangle_{\rm SNO} = \langle P_{ee}\rangle_{\rm SK} \equiv \langle P_{ee}\rangle \ ,$$

allowing a reduction to only two unknowns ($\langle P_{ee}\rangle$, f_B). The corresponding constraints placed by the current SK and SNO data are shown in Fig. 2 [17]. The data prefer $f_B \sim 1$, in agreement with the SSM expectation of [14], and clearly indicate that $\langle P_{ee}\rangle < 1$ with a significance greater than 3σ.[2] Such conclusions are strictly model-independent: no a priori assumption has been made on the SSM (i.e., on f_B) or on the energy dependence of $P_{ee}(E_\nu)$.

[2] Within $\pm 3\sigma$, it is $f_B = 1.03^{+0.50}_{-0.58}$ and $\langle P_{ee}\rangle = 0.34^{+0.61}_{-0.18}$.

2.2. Active ν oscillations

Since the model-independent analysis suggests the validity of both the SSM and the oscillation hypothesis, it makes sense *to assume* the SSM ν fluxes as input, and to calculate the oscillation probability in the simplest case of 2ν oscillations (described by the mass-mixing parameters $\delta m^2 = m_2^2 - m_1^2$ and $\omega = \theta_{12}$). The comparison with the available solar neutrino data gives, through a χ^2 statistics, allowed regions in the plane $(\delta m^2, \tan^2\omega)$. In the analysis, it is useful to include also CHOOZ reactor data [18], which are relevant to bound high values of δm^2.

Figure 1 shows the results of a global pre-SNO data analysis [17]. There are several (almost) disconnected allowed regions in the mass-mixing plane, usually called—in the solar ν jargon—as: Small Mixing Angle (SMA) at $\delta m^2 \sim 10^{-5}$ eV^2 and $\tan^2\omega \sim 10^{-3}$; Large Mixing Angle (LMA) at $\delta m^2 \sim 10^{-4}$ eV^2 and $\tan^2\omega \sim O(1)$; Low δm^2 (LOW) at $\delta m^2 \sim 10^{-7}$ eV^2 and $\tan^2\omega \sim 1$; and multiple Vacuum Oscillation (VO) solutions at large mixing and $\delta m^2 \sim O(10^{-9})$ eV^2, possibly connected to the the LOW solutions through intermediate Quasi Vacuum Oscillation (QVO)

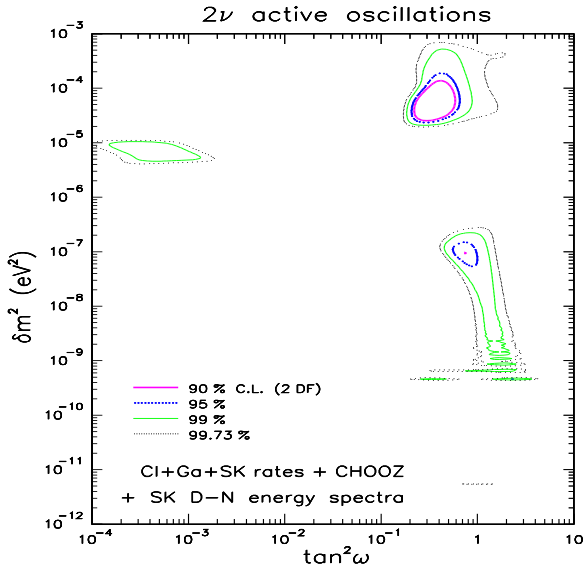

Figure 3. Global analysis of pre-SNO solar neutrino data: Favored regions in the plane of the 2ν mass-mixing oscillation parameters [17].

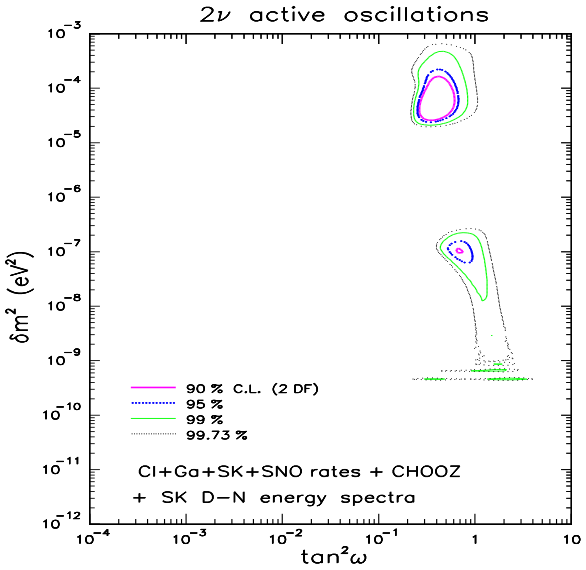

Figure 4. Global analysis of post-SNO solar neutrino data [17]. Notice that only solutions at large mixing survive.

solutions at $\delta m^2 \sim O(10^{-8})$ eV^2. The vertical "gap" at large mixing for $\delta m^2 \sim 10^{-6}$–10^{-5} eV^2 is mainly due to nonobservation of Earth matter effects at SK [12]. The horizontal gap between the SMA and the LMA regions is kept stable by SK spectral data.

Notice that, although pre-SNO data cannot exclude small mixing cases (SMA), they globally show a preference for large mixing [$\tan^2\omega \sim O(1)$]), mainly driven by SK spectral data [12,17]. The preference for large mixing is strengthened in the post-SNO analysis, as shown in Fig. 4. Indeed, the SMA solution disappears at $\sim 3\sigma$ (while the LMA one provides the best fit): a very important consequence of the first SNO CC data. The reason is the following: The SMA solution in Fig. 3 typically predicts values of $\langle P_{ee}\rangle$ larger than those favored in Fig. 2. In order to adapt to relatively low values of P_{ee}, the SMA solutions tends to move rightwards, where the nonadiabatic ν_e suppression is stronger and energy spectrum distortions are larger; in doing so, however, the SMA solution gets in conflict with the nonobservation of spectral distortions in SK, and becomes strongly disfavored in the global fit.

Similar results have been obtained in [19]. The extension to 3ν oscillations, within phenomenological bounds, does not significantly alter the emerging post-SNO global picture [20].

The surviving large-mixing solutions in Fig. 4 will soon be tested in upcoming experiments. In particular, KamLand [21] will probe the LMA solution through reactor ν disappearance over long baselines, while the Borexino solar ν experiment [22,23] will probe the LOW and (Q)VO solutions through day-night and seasonal variation effects, respectively. A confirmation of the current best-fit solution (LMA) would be extremely important for the physics potential of planned ν factory [24] or superbeam [25] projects.

2.3. Fate of the sterile neutrino

The SNO-SK data comparison provides model-independent evidence for ν_e oscillations into active species [8,10]. Can one exclude additional transitions of solar ν_e to a sterile state ν_s?

The analysis in [26] seems to show that a large ν_s component can be tolerated, provided that f_B is significantly increased: then $\nu_e \to \nu_s$ oscillations would make the extra B ν flux unobservable in SNO and SK. However, the analysis in [27] shows that, even with unconstrained ^{8}B neutrino

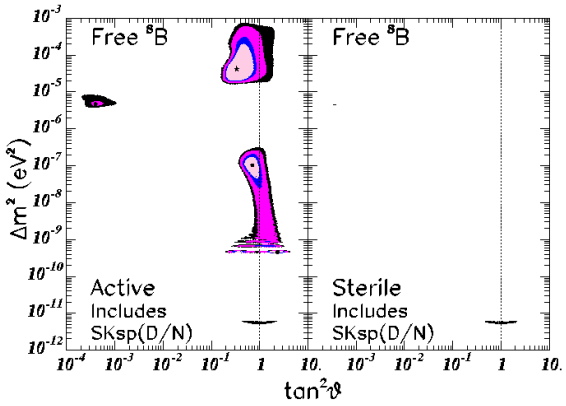

Figure 5. Comparison of solutions for ν_e oscillations into active states (left) or sterile state (right), with free f_B. The active case provides a much better fit to the data [27].

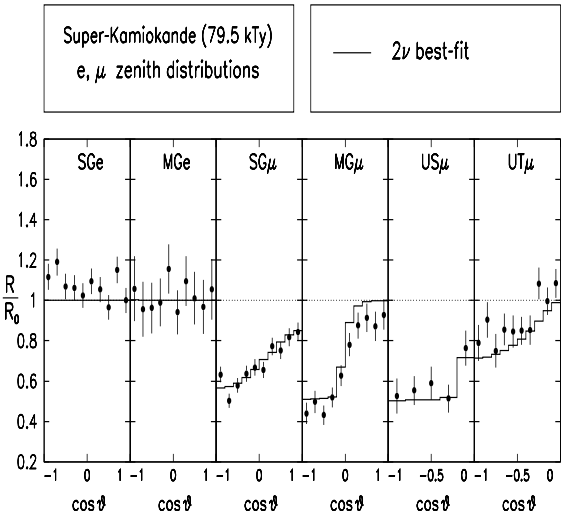

Figure 6. Best-fit predictions for normalized SK lepton (e, μ) rates R/R_0 for two-family $\nu_\mu \to \nu_\tau$ oscillations (solid histograms) in terms of the lepton zenith angle ($\cos\theta$). The no-oscillation case corresponds to $R/R_0 = 1$ (dotted line). Dots with error bars represent SK data $\pm 1\sigma_{stat}$ (SG=sub-GeV, MG=multi-GeV, US=Upward-stopping, UT=Upward-throughgoing). See also [28] for details.

flux, meaningful upper limits can be put on the ν_s admixture, since for large-amplitude $\nu_e \to \nu_s$ oscillations the global fit becomes always worse (see Fig. 5). The difference in the results can be traced [27] to the role of SK day-night spectral data, which are used in [27] but not in [26].

In any case, it can be safely concluded that there is no evidence in favor of additional ν_s mixing, although subdominant $\nu_e \to \nu_s$ transitions cannot be excluded within the still large uncertainties. The limiting case of pure $\nu_e \to \nu_s$ is strongly disfavored after SNO: accepting this case would be equivalent to assume the the SNO-SK rate difference is a mere $\sim 3\sigma$ stat. fluctuation.

3. ATMOSPHERIC NEUTRINOS

The evidence for dominant $\nu_\mu \to \nu_\tau$ oscillations in atmospheric neutrinos is robust. Figure 6 shows that the neutrino-induced lepton events in SK, spanning 4 orders of magnitude in energy E and three orders of magnitude in ν pathlength L, are perfectly described by the simple hypothesis of 2ν oscillations. The best-fit mass-mixing parameters, within a factor of about two, are stable around $m^2 = m^2_3 - m^2_{1,2} \equiv m^2 \simeq 3 \times 10^{-3}$ and $\tan^2\psi \equiv \tan^2\theta_{23} \simeq 1$ [1,28].

However, it is important to keep in mind that two important pieces of information are still "hidden" in the data: A clear observation of ν_τ appearance (for which SK can only provide interesting—but not really decisive—hints [1]) and the observation of a real "oscillatory" pattern (disappearance + reapperance). The first issue will be attacked by the CERN-to-Gran Sasso experiment OPERA [29], and the second by new long-baseline or atmospheric experiments, probing $\nu_\mu \to \nu_\mu$ disappearance with higher L/E resolution [1,29,30].

Let us now consider some current topics about the dominant $\nu_\mu \to \nu_\tau$ channel and about subdominant effects due to either extra states (ν_e or ν_s) or new interactions.

3.1. Dominant $\nu_\mu \to \nu_\tau$ oscillations

The stability of $\nu_\mu \to \nu_\tau$ oscillations as the dominant mechanism for atmospheric ν_μ disappearance is guaranteed by several independent facts: (i) nonobservation of matter effects associated to possible large ν_e or ν_s admixture [1]; (ii) strong upper bounds on additional ν_e mixing from negative CHOOZ reactor searches [18,2];

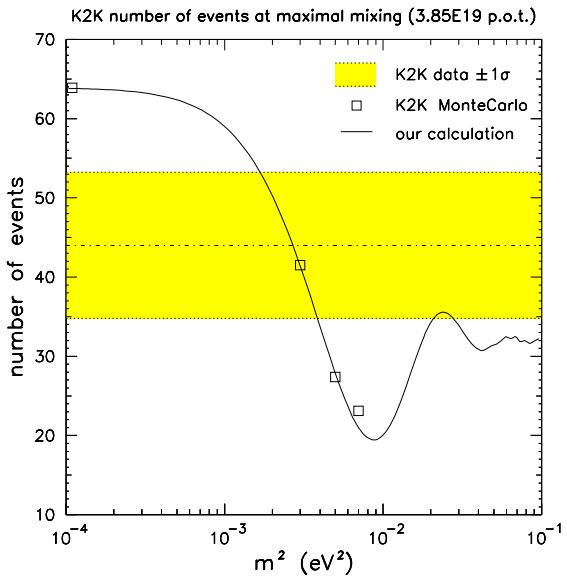

Figure 7. K2K number of events as a function of the squared mass difference m^2 for maximal $\nu_\mu \to \nu_\tau$ mixing. Horizontal band: K2K data [4]. Solid curve: Expectations in the presence of oscillations [5].

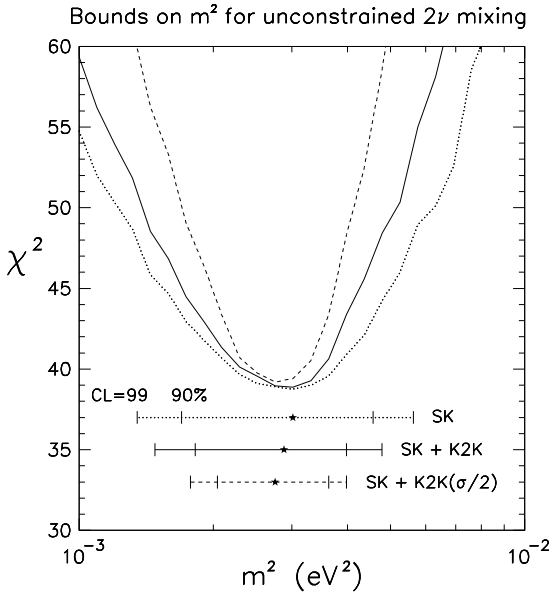

Figure 8. Results of the χ^2 analysis of SK atmospheric and K2K accelerator data in terms of the leading mass difference m^2 (for unconstrained 2ν mixing). Increasingly tighter bounds are obtained by adding to SK data the K2K data, and eventually by halving the K2K errors [5].

(iii) nonobservation of NC event suppression due to possible $\nu_\mu \to \nu_s$ in SK [18]; (iv) hints of ν_τ appearance in SK [1]; (v) generally poorer fits provided by alternative ("exotic") explanations [1], with the possible exception of a decoherence model [31]. The stability of the best-fit parameters, on the other hand, is guaranteed by the strong disappearance effect observed in the MGμ sample of SK ($E \sim$ few GeV, see Fig. 6): the onset of disappearance at the horizon (fixing the length scale L) determines the squared mass difference $m^2 \sim E/L$, while the maximum suppression of the upward muon rate ($\sim 1/2$) forces the mixing amplitude $\sin^2 2\psi$ to be nearly maximal.

3.2. Impact of K2K

The KEK-to-Kamioka (K2K) long-baseline ν experiment ($L = 250$ km) aims to verify the SK atmospheric ν anomaly through disappearance of low-energy (> 1 GeV) accelerator ν_μ's. The recent K2K data [4] (44 events observed against 64 expected) already suggest that the null hypothesis of no oscillations is rejected at 97% C.L. [4].

One can make a further step and analyze the consistency and the impact of K2K data in the context of the $\nu_\mu \to \nu_\tau$ oscillation scenario [5].

Figure 7 shows the number of events expected in K2K (solid curve) as a function of m^2 (for maximal mixing, $\tan^2 \psi = 1$), as compared with the K2K data (1σ allowed band). The theoretical curve crosses the central value of the band at $m^2 \sim 2.5 \times 10^{-3}$ eV^2, in agreement with the value derived from SK atmospheric ν data. Therefore, K2K supports the same $\nu_\mu \to \nu_\tau$ oscillation scenario favored by atmospheric neutrino experiments, and it makes sense to combine SK and K2K data in a global analysis (dominated, of course, by the more accurate SK data).

The results are shown in Fig. 8, in terms of bounds on m^2 from SK only, from SK+K2K, and from SK+K2K with halved K2K errors. It can be seen that K2K can appreciably tighten both the lower and the upper bound on m^2. Strengthening the lower bound is particularly important for the new generation of accelerator experiments with longer baselines [29], which would rapidly loose sensitivity to oscillation effects for m^2 approaching $\sim 1 \times 10^{-3}$ eV^2.

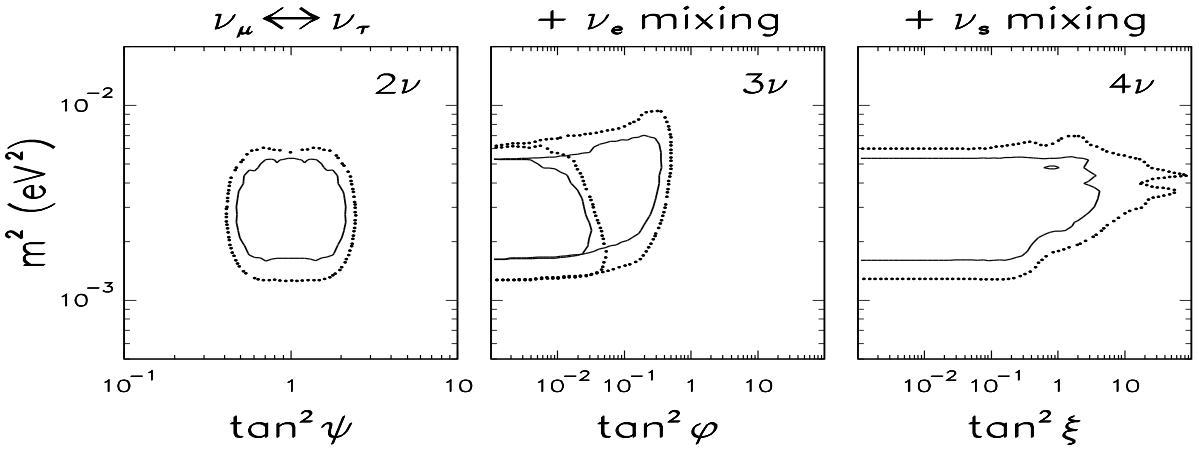

Figure 9. Bounds on atmospheric neutrino oscillation parameters $(m^2, \tan^2\psi)$ for dominant flavor states ν_μ, ν_τ (left panel), and upper bounds on additional mixing with extra states, parametrized through $\tan^2\phi$ for ν_e (middle panel, with and without CHOOZ), and through $\tan^2\xi$ for ν_s (right panel). The middle and left panels are relevant for scenarios with three and four neutrino mixing [28].

3.3. Subdominant oscillations from extra states

It is natural to assume that at least one extra state (ν_e) can play a role besides dominant $\nu_\mu \to \nu_\tau$ oscillations (3ν mixing). A possible light sterile state ν_s might also participate to oscillations in extended 4ν scenarios [32]. In both cases, the standard L/E dependence of the $\nu_\mu \to \nu_\tau$ oscillation phase is modified by the so-called Mikheyev-Smirnov-Wolfenstein (MSW) matter effects in the Earth. Simbolically,

$$\text{Oscillation phase} \propto [L/E] \oplus [\text{MSW}] \ .$$

Nonobservation of deviations from the standard L/E dependence in SK places significant constraints on additional mixing of $\nu_{\mu,\tau}$ with additional flavor states. The results are shown in Fig. 9, as we now discuss.

3.3.1. Additional ν_e mixing

The middle panel of Fig. 9 shows the bounds on additional ν_e mixing, expressed in terms of the leading squared mass difference m^2 and of $\tan^2\phi$, where $\phi = \theta_{13}$ in usual 3ν mixing notation. The looser bounds in the panel arise from the absence of observed MSW effects and of distortions of the electron samples in SK (see also Fig. 6). The tighter bounds refer to the SK+CHOOZ combination, dominated by the CHOOZ nonobservation of $\bar{\nu}_e$ disappearance.

Altogether, SK+CHOOZ set an upper bound of a few % on additional ν_e mixing. Such bound is probably too tight to allow detection of residual matter effects with higher SK statistics [28,33]. Establishing a nonzero value for $\phi = \theta_{13}$ is a major challenge for future neutrino oscillation experiments, with far-reaching consequences also for non-oscillatory probes of the neutrino mass and mixing [34] and for model building and leptonic CP violation [35].

3.3.2. Additional ν_s mixing

In this case, matter effects are typically somewhat weaker than for ν_e mixing, and there is no analogous of the CHOOZ experiment. Therefore, the upper bounds on ν_s mixing (parametrized in Fig. 9 in terms of a suitable angle ξ, see [28]), are weaker than the previous ones for ν_e mixing.

However, it should be added that the limits in the right panel of Fig. 9 can be improved by adding: further SK data on NC enriched events [1]; SK hints for τ appearance [1]; MACRO muon data [2,36]. Our educated guess is that a global combination of all such data would limit subdominant ν_s mixing below 20–30%.

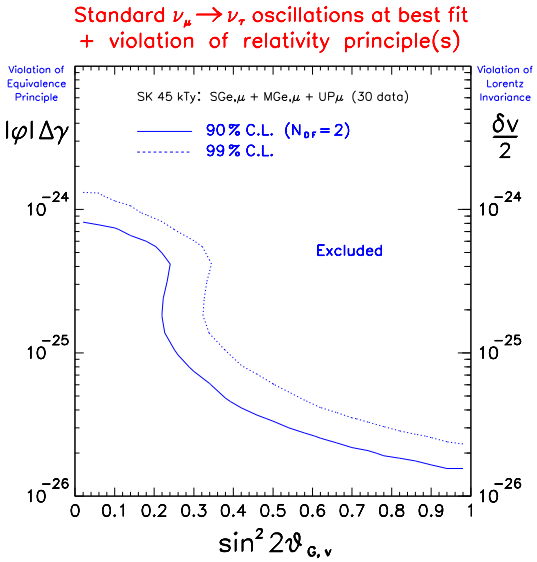

Figure 10. Standard $\nu_\mu \to \nu_\tau$ mass-mixing oscillations plus violations of relativity principles: Upper bounds from SK data. See [37] for details.

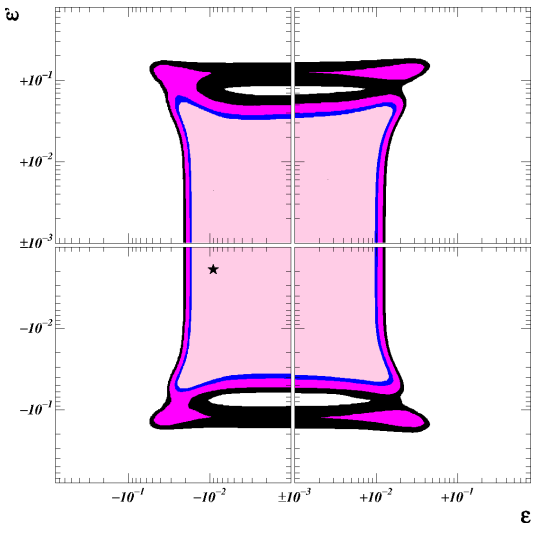

Figure 11. Standard $\nu_\mu \to \nu_\tau$ mass-mixing oscillations plus extra four-fermion interactions: Upper bounds from SK data. See [39] for details.

3.4. Subdominant oscillations from extra interactions

The standard L/E oscillation phase of atmospheric $\nu_\mu \to \nu_\tau$ oscillations can be modified not only by extra states, but also by extra (nonstandard) interaction of $\nu_{\mu,\tau}$ with a "generalized" background, which can be either the Earth matter, or the local gravitational field, or the spacetime itself. A large class of nonstandard interactions predict extra oscillations phases with a power-law dependence on energy [37]

$$\text{Oscillation phase} \propto [L/E] \oplus [L/E^n] \ .$$

with integer n. The broad L/E range spanned by SK sets severe limits on the amplitude of nonstandard ($n \neq -1$) phases, as we show for two representative cases. Future (very) long baseline accelerator experiments will not easily improve such limits [38], due to the their much narrower range of L/E probed.

3.4.1. Additional VEP, VLI

Violations of the equivalence principle (VEP), i.e., different coupling of $\nu_{\mu\tau}$ to gravity, can generate flavor oscillations. Violations of Lorentz invariance (VLI), i.e., different limiting speeds for $\nu_{\mu,\tau}$ can also generate oscillations. Both cases generate extra oscillation phases with $n = +1$ (phase $\propto L \cdot E$) [37]. When added on top of standard $\nu_\mu \to \nu_\tau$ transitions, such hypothetical violations are found to worsen the fit to SK data. The lack of evidence in favor of them allows to set strong upper bounds to their amplitude, as shown in Fig. 10 [37]. Such bounds are much tighter than the corresponding ones derived in another "oscillation laboratory", namely, the kaon system.

3.4.2. Additional FCNC, FDNC

Additional NC-type, four-fermion interactions can arise in SUSY models with R-parity breaking, leading to flavor-changing (FC) or flavor-diagonal (FD) neutrino transitions in matter. The amplitudes of such interactions are usually parameterized as "fractions" (ϵ's) of the standard Fermi amplitude G_F. Their effect on oscillations is to produce energy-independent ($n = 0$) extra phases. No evidence is found for such phases, and upper bounds on the ϵ's have been recently derived in [39]. Figure 11 reports the basic results of [39]: nonstandard interactions cannot exceed a few percent strength (in units of G_F).

4. COMMENTS ON 4ν MIXING

While solar, atmospheric, and CHOOZ data can be accommodated in a scenario involving only the three known neutrinos [35,40], problems arise when one tries to embed also the controversial evidence for oscillations in the $\nu_\mu \to \nu_e$ channel found by LSND [13], which is not supported (but not totally excluded) by the competing Karmen experiment (see Fig. 12). The evidence is characterized by small mixing and a large squared mass difference, which is incompatible with solar and atmospheric neutrino parameters, unless a fourth (sterile) neutrino state is introduced [32].

Two four-neutrino mass spectra can be envisaged : one with three close states and a lone state (3+1) [41], and one with two separated doublets (2+2) [32]. Such spectra can, in principle, accommodate the three independent square mass differences needed to drive solar, atmospheric, and LSND oscillations. However, mixing angles turn out to be difficult to arrange without spoiling the agreement with some data.

In the 2+2 case, it turns out that the fractional admixture of ν_s in the "solar" and "atmospheric" doublets must add up to one. Symbolically:

$$2+2: \ [\nu_s]_{\rm sol} + [\nu_s]_{\rm atm} = 1 \ .$$

However, the best fits to $[\nu_s]_{\rm sol}$ and $[\nu_s]_{\rm atm}$ are close to zero (as we have seen in Sec. 2.3 and 3.3.2, respectively), so that the above sum rule cannot be satisfied unless either $[\nu_s]_{\rm sol}$ or $[\nu_s]_{\rm atm}$ are pushed to their upper limits at 2–3σ [42].

In the 3+1 case, it turns out that the LSND appearance probability $P_{\mu e}$ is proportional to the ν_μ disappearance probability (constrained by the CDHSW accelerator experiment) and to the ν_e disappearance probability (constrained by the Bugey reactor experiment). Symbolically:

$$3+1: \ P_{\mu e}^{\rm LSND} \propto P_{\mu\mu}^{\rm CDHSW} \cdot P_{ee}^{\rm Bugey} \ .$$

Since both factors on the r.h.s. are experimentally consistent with zero, the expected LSND probability is doubly suppressed, and it turns out to be too small to fit the observed data [36].

In conclusion, the LSND evidence does not seem to fit well in 4ν schemes: tension is generated between solar and atmospheric data in the 2+2 case, and between accelerator and reactor data in the 3+1 case. This tension is not strong enough, however, to exclude 4ν mixing with high confidence yet [36].

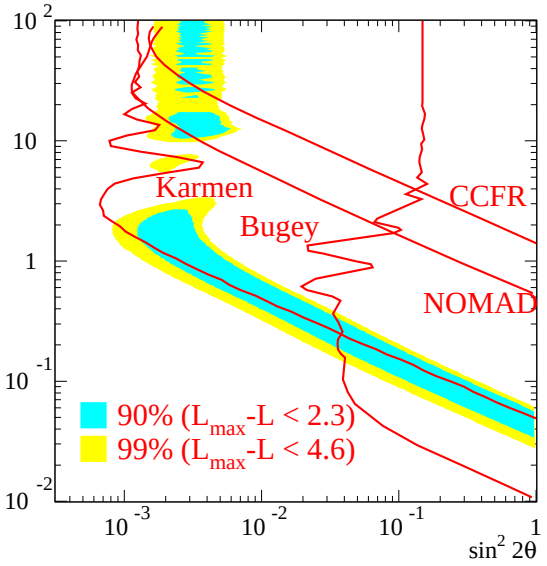

Figure 12. LSND allowed region (shaded) *vs* regions excluded by other experiments in the $\nu_\mu \to \nu_e$ mass-mixing plane.

In any case, independently from the above (model-dependent) arguments, the LSND issue will be soon settled by the MiniBoone experiment [43]. Disconfirmation of LSND would reinforce the standard 3ν oscillation interpretation of solar and atmospheric ν data. A confirmation would instead imply a serious global re-examination of the oscillation evidence, in order to find new ways to make LSND compatible with world data.

5. SUMMARY

We have reviewed recent topics in the neutrino oscillation phenomenology. The solar neutrino evidence for active ν oscillations is significantly strengthened by SNO data as compared to SK data, independently on specific solar or oscillation models. The post-SNO oscillation fit strongly favors large-mixing solutions, with a preference for relatively high values of the neutrino squared mass difference (LMA solution). Solar neutrinos do not provide evidence for a sterile ν admixture, although a subdominant ν_s component can be

easily tolerated. Atmospheric neutrinos are beautifully explained by dominant $\nu_\mu \to \nu_\tau$ oscillations. Preliminary K2K data are consistent with this interpretation. Upper bounds can be placed on subdominant admixtures of extra states (ν_e or ν_τ) and on subdominant contributions of extra interactions (beyond the standard model). Solar and atmospheric neutrino data can be easily embedded in a 3ν mixing scenario. However, when one tries to add a fourth sterile neutrino to embed also the LSND data, tension arises between subsets of data. A series of new experiments will greatly improve and refine the current picture of neutrino mass and mixing in the near future (or in the next decade at most), and will possibly set new challenges for the phenomenological interpretation and for model building.

Acknowledgments

This work is supported by the Italian INFN and MIUR under the "Astroparticle Physics" project.

REFERENCES

1. Y. Totsuka, these Proceedings.
2. E. Scapparone, these Proceedings.
3. D. Petyt, these Proceedings.
4. T. Hasegawa, these Proceedings.
5. G.L. Fogli, E. Lisi, and A. Marrone, hep-ph/0110089.
6. G. Cattadori, these Proceedings.
7. V. Vermul, these Proceedings.
8. A. McDonald, these Proceedings.
9. J.N. Bahcall, Phys. Rev. C **65**, 015802 (2002).
10. SNO Collaboration, Phys. Rev. Lett. **87**, 071301 (2001).
11. I. Lawson, these Proceedings.
12. SK Collaboration, Phys. Rev. Lett. **86**, 5651 (2001); *ibidem*, p. 5656.
13. LSND Collaboration, Phys. Rev. D **64**, 112007 (2001).
14. J.N. Bahcall, M.H. Pinsonneault, and S. Basu, Astrophys. J. **555**, 990 (2001).
15. F.L. Villante, G. Fiorentini, and E. Lisi, Phys. Rev. D **59**, 013006 (1999).
16. G.L. Fogli, E. Lisi, A. Palazzo, and F.L. Villante, Phys. Rev. D **63**, 113016 (2001).
17. G.L. Fogli, E. Lisi, D. Montanino, and A. Palazzo, Phys. Rev. D **64**, 093007 (2001).
18. CHOOZ Collaboration, Phys. Lett. B **466**, 415 (1999).
19. J.N. Bahcall *et al.*, JHEP **0108**, 014 (2001); A. Bandyopadhyay *et al.*, Phys. Lett. B **519**, 83 (2001); P.I. Krastev and A.Yu. Smirnov, hep-ph/0108177; M.V. Garzelli and C. Giunti, JHEP **0112**, 017 (2001); P. Creminelli *et al.*, hep-ph/0102234 v2.
20. G.L. Fogli *et al.*, Proceedings of the Workshop "Neutrino Oscillations in Venice", July 2001, edited by M. Baldo-Ceolin, to appear.
21. S. Schoenert, these Proceedings.
22. T. Shut, these Proceedings.
23. V. Antonelli, these Proceedings.
24. F. Dydak, these Proceedings.
25. T. Kobayashi, these Proceedings.
26. V.D. Barger, D. Marfatia, and K. Whisnant, hep-ph/0106207.
27. J. Bahcall *et al.*, first Ref. of [19]; see also M.C. Gonzalez-Garcia, M. Maltoni, and C. Pena-Garay, hep-ph/0111150.
28. G.L. Fogli, E. Lisi, and A. Marrone, Phys. Rev. D **64**, 093005 (2001).
29. J. Schneps, these Proceedings.
30. T. Tabarelli, these Proceedings.
31. E. Lisi, A. Marrone, and D. Montanino, Phys. Rev. Lett. **85**, 1166 (2000).
32. S.M. Bilenky, C. Giunti, and W. Grimus, Prog. Part. Nucl. Phys. **43**, 1 (1999).
33. O. Peres, these Proceedings.
34. H.V. Klapdor-Kleingrothaus, these Proc.
35. P. Langacker, these Proceedings.
36. M. Maltoni, T. Schwetz, and J.W.F. Valle, hep-ph/0112103.
37. G.L. Fogli, E. Lisi, A. Marrone, and G. Scioscia, Phys. Rev. D **60**, 053006 (1999), and refs. therein.
38. R. Zukanovich-Funchal, these Proceedings.
39. N. Fornengo *et al.*, Phys. Rev. D **65**, 013010 (2002).
40. G.L. Fogli *et al.*, hep-ph/0104221.
41. O.L.G. Peres and A.Yu. Smirnov, Nucl. Phys. B **612**, 59 (2001).
42. M.C. Gonzalez-Garcia, M. Maltoni, and C. Pena-Garay, Phys. Rev. D **64**, 093001 (2001).
43. R. Stefansky, these Proceedings.